



Design, optimization, and evaluation of ezetimibe solid supersaturatable self-nanoemulsifying drug delivery for enhanced solubility and dissolution

Rajendra Narayan Dash¹ · Habibuddin Mohammed²  · Touseef Humaira²

Received: 29 March 2015 / Accepted: 23 November 2015 / Published online: 30 November 2015
© The Korean Society of Pharmaceutical Sciences and Technology 2015

Abstract This study was intended to develop a solid supersaturatable self-nanoemulsifying drug-delivery system (solid S-SNEDDS) to improve the solubility and dissolution of a poorly water-soluble drug ezetimibe. Self-nanoemulsifying drug delivery system (SNEDDS) preconcentrate was systematically optimized by a central composite design ($\alpha = 1.682$). The optimized SNEDDS preconcentrate consisted of Captex 355 (30 % w/w), Cremophor RH40 (40 % w/w) and Imwitor 988 (30 % w/w). Saturation solubility of ezetimibe in the optimized SNEDDS preconcentrate was found to be 90.62 mg/ml. HPMC-E5 (5 % w/w) and ezetimibe (90 % saturation solubility level) were added to the SNEDDS preconcentrate to form a supersaturatable SNEDDS (liquid S-SNEDDS). Dilution of liquid S-SNEDDS resulted in a nanoemulsion having a mean droplet size of 27.3 nm. TEM studies of diluted liquid S-SNEDDS confirmed uniform shape and size of the droplets. The liquid formulation was adsorbed onto microcrystalline cellulose and talc to form a solid S-SNEDDS. In vitro supersaturation test of solid S-SNEDDS showed a higher ezetimibe concentration (that retarded precipitation of ezetimibe at least up to 60 min) in

comparison to the solid-SNEDDS (without HPMC-E5). PXRD studies of the precipitates collected from the in vitro supersaturation test, revealed the presence of amorphous ezetimibe. DSC and SEM results indicated that the presence of ezetimibe in an amorphous and molecular dispersed state within the solid S-SNEDDS. In vitro release (in 15 min) of ezetimibe from solid S-SNEDDS improved by 1.17, 1.69, and 13.21-fold as compared with solid-SNEDDS, commercial product, and the free drug (powder), respectively.

Keywords Central composite design · Solid S-SNEDDS · Supersaturation · Solubility enhancement · Dissolution enhancement

Introduction

Ezetimibe is a hypo-lipidemic agent that specifically inhibits the absorption of cholesterol from the intestine, leading to a decreased cholesterol delivery to the liver (Sweetman 2009). It is a poorly water-soluble drug having a log P of 4.52 (Lestari Maria et al. 2009) and exhibits intersubject variability in oral bioavailability (35–60 %) (Kosoglou et al. 2005). Owing to the hydrophobic nature of ezetimibe, various strategies have been employed in order to improve its solubility such as cyclodextrin complex (Patel et al. 2008), solid dispersion (Parmar et al. 2011; Sancheti et al. 2009), liquid–solid compact (Khanfar et al. 2013), nanocrystal (Gulsun et al. 2011), drug loaded mesoporous silica (Kiekens et al. 2012), nanoparticles (Pandya and Patel 2011), nanoemulsion (Bali et al. 2010), self-nanoemulsifying drug delivery system (SNEDDS) (Dabhi et al. 2011; Dixit and Nagarsenker 2008) and supersaturatable SNEDDS (Bandyopadhyay et al. 2014).

Electronic supplementary material The online version of this article (doi:10.1007/s40005-015-0225-9) contains supplementary material, which is available to authorized users.

✉ Habibuddin Mohammed
drhabib21@gmail.com

¹ Alliance Institute of Advanced Pharmaceutical & Health Sciences, Plot No. 64, Survey No. 145, Sardar Patel Nagar, Kukatpally, Hyderabad, Telangana 500072, India

² Adept Pharma and Bioscience Excellence Private Limited, Corporate Office: 10-3-561/3/A/102, Vijayanagar Colony, Hyderabad, Telangana 500057, India

Lipid suspensions, solutions and emulsions have all been used to enhance the solubility of poorly soluble drugs (Pouton 2000). More recently, there has been a growing focus on the utility of the self-nanoemulsifying drug delivery system (SNEDDS) (Pund et al. 2014). SNEDDS is a thermodynamically stable, an isotropic mixture of oil, surfactant, co-surfactant, and drug that forms oil-in-water nanoemulsion with a droplet size of less than 100 nm (Bali et al. 2011).

SNEDDS offers the unique benefits of improving drug absorption through several ancillary mechanisms, namely; (i) drug solubilization, (ii) inhibition of p-glycoprotein (P-gp) mediated drug efflux, (iii) promotion of lymphatic transport while avoiding first-pass metabolism, (iv) improved permeability across the gastrointestinal (GI) membrane (Dash et al. 2015a; Pund et al. 2014). However, SNEDDS suffers from potential obstacles such as lower drug loading capacity and precipitation of the drug upon dilution (Mohsin et al. 2009).

To overcome such difficulties there has been an increasing focus towards the application of the supersaturatable SNEDDS (S-SNEDDS) (Bandyopadhyay et al. 2014; Dash et al. 2015b). S-SNEDDS contains a polymeric precipitation inhibitor (PPI) in addition to the typical composition of SNEDDS. The PPI adsorbs onto the hydrophobic nuclear surface, act as a barrier for the nucleation process that is essential for the crystal formation and crystal growth. Further, this prevents the drug from precipitating out of the solution, thus temporarily maintaining a metastable supersaturated state (Gao et al. 2009). Consequently, the stabilization of the supersaturated state can provide an effective solution for the solubility limited oral bioavailability of lipophilic drugs (Brouwers et al. 2009).

Moreover, it is important to convert the liquid S-SNEDDS to a solid dosage form having better transportability, high stability, cost effective manufacturing, and above all, the increased therapeutic success owing to its better patient compliance (Dash et al. 2015a; Hu et al. 2012). Hence, the present research work aims at developing a stable, solid S-SNEDDS of ezetimibe that would generate a supersaturated state upon dilution. Simultaneously, it was hypothesized that the generation of a nanoemulsion following dilution of S-SNEDDS could provide a large interfacial surface area for enhanced solubility and dissolution of ezetimibe.

Materials and methods

Materials

Ezetimibe was a generous gift from Alembic Ltd., Vadodara, India. Medium chain tri-glycerides (MCT) such as Captex 300[®], Captex 355[®] and medium chain mono-

glycerides (MCM) Capmul MCM[®] were kindly provided by Abitec Corp., Janesville, USA. Solutol HS15[®] (Polyglycol mono and di-esters of 12-hydroxy stearic acid) and Cremophor RH40[®] (polyethylene glycol-40 hydrogenated castor oil) were provided by BASF SE, Ludwigshafen, Germany. Labrafac lipophile WL1349TM (MCT), Labrafac PGTM (propylene glycol dicaprylocaprate), and Labrasol[®] (PEG-8 glyceryl caprylate) were kind gifts from Gattefosse Corp. (Saint-Priest, France). Miglyol 812 N[®] (MCT) and Imwitor 988[®] (MCM) were obtained from Sasol olefins, GmbH, Germany. Hydroxypropyl methylcellulose of 5-cps grade (HPMC-E5) was provided by Colorcon Asia Pvt. Ltd., Mumbai, India. Hard gelatin capsule shell (size 1) was supplied by Capsugel Health Care Ltd., Mumbai, India. Tween 80, Coconut oil, Castor oil, Olive oil, Polyethylene glycol-400, Microcrystalline cellulose, and Talc were purchased from Himedia Pvt. Ltd., Mumbai, India. HPLC grade water of 18 M Ω was obtained in-house from a Direct Q-3 UV water purification system (Millipore India Pvt. Ltd., Bengaluru, India) and used in this study for the dilution of SNEDDS pre-concentrates or SNEDDS.

Solubility studies

The solubility of ezetimibe in long chain triglycerides (LCT) (Castor oil, Coconut oil, and Olive oil), MCT/synthetic oils (Labrafac lipophile WL1349, Labrafac PG, Captex 300, Captex 355, and Miglyol 812 N), optimized SNEDDS pre-concentrate, and in the water were determined in triplicate. An excess of ezetimibe was added to each vial containing 2 ml of the above vehicles. The vials were vortexed for 5 min and stirred continuously for 7 days in a water bath shaker (RSB-12, Remi, Mumbai, India) at 37 ± 0.5 °C. After a specified period, all the samples were centrifuged at 5000 rpm for 15 min (RM-12C, Remi, Mumbai, India) and the supernatant was analyzed for ezetimibe content by in-house developed RPHPLC method (Dash et al. 2014). The HPLC system (series 200, Perkin Elmer, USA) was consisted of a quaternary pump, auto sampler, UV-Vis detector and temperature-controlled oven. Analysis of ezetimibe was performed at 35 ± 2 °C using Luna C8 (100 \times 4.6 mm, 3 μ m) analytical column (Phenomenex, USA). The mobile phase employed for elution was acetonitrile: potassium dihydrogen phosphate buffer (pH 3.5, 20 mM) (45:55, v/v) with a flow rate of 0.8 ml/min. The detection wavelength and injection volume were kept at 232 nm and 20 μ l, respectively.

Screening of surfactants and co-surfactants

Surfactant and co-surfactant were selected based upon their emulsifying ability over solubilizing property. Surfactants (Cremophor RH40, Solutol HS15, Labrasol, Cremophor EL, and Tween 80) and co-surfactants (Imwitor 988,

Capmul MCM, Capmul PG8, and Polyethylene glycol 400 were screened as per the method described in our previous report (Dash et al. 2015a).

Ternary phase diagram studies

Ternary phase diagram studies were performed on the selected oil, surfactant, and co-surfactant to locate the region of nanoemulsion. A series of mixtures (2 g) was prepared with varying concentration of oil (10–80 parts w/w), surfactant (10–80 parts w/w), and co-surfactant (10–50 parts w/w). For any mixture, the sum of oil, surfactant, and co-surfactant was 100 %. Each mixture (100 mg) was introduced in 20 ml water in a glass beaker, and the contents were gently mixed (at 50 rpm) using a magnetic stirrer (2MLH, Remi, Mumbai, India). The dispersion having a clear or slightly bluish appearance was considered in the region of nanoemulsion (Basalious et al. 2010).

Optimization of SNEDDS preconcentrate by experimental design

A three-factor, five-level circumscribed central composite design (CCD) with $\alpha = 1.68$ was used to optimize SNEDDS preconcentrate (Hu et al. 2012). The term “ α ” is the measure of distance between each axial point and center of the CCD (Montgomery 2013). The studied factors were Oil/Captex 355 (X1), Surfactant/Cremophor RH40 (X2), and Co-surfactant/Imwitor 988 (X3). The responses such as mean droplet size (nm) (Y1), turbidity (NTU) (Y2), and transmittance (%) (Y3) were evaluated. The experimental studies were designed using Minitab[®] version 16 (Minitab, Inc. UK). Studies were randomized to reduce bias. As per the experimental plan, 20 SNEDDS preconcentrates were prepared and assessed for the responses after diluting 500 times with water. The concentrations of X1, X2 and X3 were expressed as percentage by weight while analyzing the experimental result by Statistica[®] version 10.0 (Stat soft, Inc., OK, USA) and Design Expert[®] version 8.0 (Stat-Ease, MN, USA). A second-order polynomial regression model (Eq. 1) that satisfies the linear, quadratic, and interaction effects of studied factors were built for the individual response as follows.

$$Y = \beta_0 + \beta_1 (X_1) + \beta_2 (X_2) + \beta_3 (X_3) + \beta_{11} (X_1)^2 + \beta_{22} (X_2)^2 + \beta_{33} (X_3)^2 + \beta_{12} (X_1X_2) + \beta_{13} (X_1X_3) + \beta_{23} (X_2X_3) \quad (1)$$

where Y , the response; β_0 , arithmetic means for a particular response; β_1 , β_2 , and β_3 are the estimated coefficients for X_1 , X_2 , and X_3 respectively. The models were validated by analysis of variance (ANOVA). Statistical P value < 0.05 was considered as significant.

Formulation of liquid S-SNEDDS

Ezetimibe (at 90 % saturation solubility level) was added to a series of optimized SNEDDS preconcentrates (10 g) kept in dust-free glass vials. The vials were vortex mixed with a Cyclo-mixer (CM101, Remi, Mumbai, India) until a clear solution was obtained. Variable amounts of HPMC-E5 at a concentration of 0, 0.5, 1, 3, 5, 7.5, and 10 % w/w were added to the above drug-loaded optimized SNEDDS preconcentrates and mixed using the Cyclo-mixer (CM101, Remi, Mumbai, India) to obtain uniform suspensions.

Characterization of liquid S-SNEDDS

Thermodynamic stability studies

Thermodynamic stability tests such as centrifugation, heating–cooling cycle, and cloud point estimation were conducted on the liquid S-SNEDDS as per the procedure stated in our previous report (Dash et al. 2015a). Liquid S-SNEDDS was verified for any sign of phase separations.

Measurement of droplet size and zeta potential

Dynamic light scattering (DLS) technique was employed to measure the mean droplet size, droplet size distribution, and zeta potentials of the diluted liquid S-SNEDDS. Briefly, 0.1 g of liquid S-SNEDDS was diluted to 50 ml with water, mixed gently, and allowed to stand for 12 h at room temperature (Dash et al. 2015a). The above-mentioned parameters for diluted liquid S-SNEDDS were measured using a Zeta potential/Particle Sizer (Nanopartica SZ100, Horiba instrument, UK).

Measurement of transmittance and turbidity

The resulting emulsions obtained after diluting liquid S-SNEDDS were assessed for percentage transmittance and turbidity by a UV–Vis spectrophotometer (T80+, PG Instrument, UK) and Digital nephlo-turbidity meter (132, Systronics India) respectively using water as blank.

Transmission electron microscopy

The morphology of nanoemulsion was observed using a transmission electron microscope (JEM-1200EX, Jeol, Japan). One drop of diluted liquid S-SNEDDS was deposited on a 200 mesh-copper grid. The grid was stained with 2 % uranyl acetate for 30 sec, dried at room temperature and observed under the electron microscope.

Formulation of solid S-SNEDDS

Adsorption technique was employed to prepare the solid S-SNEDDS. Liquid S-SNEDDS (with or without HPMCE-5) was adsorbed onto microcrystalline cellulose (Tang et al. 2008). Briefly, liquid S-SNEDDS (10 g) was poured onto microcrystalline cellulose (15 g) placed in a mortar, mixed for 5 min to obtain a homogenous mass. Talc (2 g) used as the lubricant, was added to the above mass, mixed gently, and passed through a 250- μm mesh. Similarly, respective solid S-SNEDDS blanks were prepared as per the above procedure but without using ezetimibe. The drug content was determined in each formulation by HPLC. Powder of solid S-SNEDDS equivalent to 10 mg of ezetimibe was filled into size “1” hard gelatin capsules (Capsugel, Mumbai, India), and stored at 25 °C until used for the subsequent studies.

Characterization of solid S-SNEDDS

Micromeritic properties

The flow properties of solid S-SNEDDS were determined in terms of Carr's index, Hausner's ratio, and angle of repose. Angle of repose was determined by static funnel method, whereas Hausner's ratio and Carr's index were computed from the bulk and tapped densities (Carr 1965).

In vitro supersaturation test and selection of PPI concentration

In vitro supersaturation test was performed in triplicate on the final product (solid S-SNEDDS) with varying content of HPMC-E5 as per the procedure described by Wei et al. (2012). A simulated gastric fluid containing 0.01 M HCl and 0.15 M NaCl (pH 2.0) was chosen as an in vitro medium. Solid S-SNEDDS capsules containing variable amounts of HPMC-E5 were placed in 100 ml of the test medium. The media were maintained at 37 °C and stirred continuously at 100 rpm on a magnetic stirrer (2MLH, Remi, Mumbai, India). Samples (500 μl) were withdrawn without volume replacement in 2, 5, 15, 30, 60, and 120 min and filtered through a 0.45 μm filter. The 300 μl was discarded before collecting the final 200 μl of filtrate. Further, the filtrates were analyzed for ezetimibe content by HPLC. Similarly, a control experiment was performed using a HPMC-E5 free solid S-SNEDDS blank capsule. After 24 h of the in vitro supersaturation test, precipitates were collected from the tested formulations. The crystalline property of ezetimibe in the collected precipitates was checked using powder XRD studies.

Powder XRD (PXRD) studies

The powder X-ray diffraction studies of ezetimibe, precipitates obtained from the in vitro supersaturation tests, precipitates obtained from the control experiment (blank precipitates), physical mixtures (blank precipitate spiked with a corresponding amount of ezetimibe present in the solid S-SNEDDS), and individual excipients (microcrystalline cellulose, talc, and HPMC-E5) were carried out with an X-ray diffractometer (D8 Advanced, Bruker AXS, Germany). The instrument uses a $\text{CuK}\alpha$ radiation generated at 40 kV with 40 mA current and operated over a 2 θ angle ranging from 6° to 50° at an increment of 0.1°.

Differential scanning calorimetry (DSC)

The physical state of ezetimibe, solid S-SNEDDS, solid S-SNEDDS blank, physical mixtures (solid S-SNEDDS blank spiked with the corresponding amount of ezetimibe present in the solid S-SNEDDS), and individual excipients (e.g. microcrystalline cellulose, talc, and HPMC-E5) were carried out using a thermal analyzer (Pyris 6, Perkin Elmer, USA). Samples were scanned from 40 to 320 °C at a temperature increment of 10 °C/min.

Scanning electron microscopy (SEM)

The external surface and cross-sections of ezetimibe, solid S-SNEDDS, solid S-SNEDDS blank and physical mixtures were investigated using a scanning electron microscope (S-4100, Hitachi, Japan) operated at 15 keV accelerating voltages.

Fourier transformed infrared (FTIR) spectroscopy

To observe any possible drug-excipient interaction; FTIR spectroscopic studies were conducted for ezetimibe, solid S-SNEDDS, solid S-SNEDDS blank and physical mixtures. The spectra were recorded on a FTIR spectrophotometer (Alpha-T, Bruker AXS, Germany) using pressed pellet techniques (KBr disc) over a range of 500–4000 cm^{-1} .

Comparative in vitro release studies

Comparative in vitro release studies were performed on solid S-SNEDDS capsule, solid-SNEDDS capsule (without HPMC-E5), commercial tablet (Ezedoc[®], Lupin Ltd. India), and free drug (powder), each containing 10 mg of ezetimibe. In vitro release studies were conducted as per the method described by Dixit and Nagarsenker (2008), with slight modification. These studies were carried out using a USP dissolution type I apparatus (TDT-08L, Electrolab, Mumbai, India) in 500 ml of 0.5 % (w/v)

sodium lauryl sulphate maintained at 37 ± 0.5 °C. The rotation of the basket was adjusted to 75 rpm. Aliquots of 5 ml were withdrawn in 5, 10, 15, 30, 45, 60, 75, and 90 min and replaced with fresh dissolution medium. The collected samples were diluted with mobile phase, filtered through the $0.22 \mu\text{m}$ nylon membrane, and analyzed for the drug content by HPLC.

Accelerated stability studies

Accelerated stability studies were carried out for solid S-SNEDDS as per requirement of ICH guidelines, Q1A (R2) (2003) for climatic zone IV. Three batches of solid S-SNEDDS capsules sealed in high-density polyethylene bottles were subjected to 40 ± 2 °C/ 75 ± 5 % RH up to 6 months. Samples were withdrawn after a particular time interval (0, 3, and 6 months). Samples were visually examined for physical changes and evaluated for the drug content by HPLC. Mean droplet size after nanoemulsification and percentage of drug release in 15 min ($\text{DR}_{15\text{min}}$) was measured. Similarity factor (f_2) was calculated to test the similarities of dissolution profiles.

Estimation of shelf life of solid S-SNEDDS

For estimating shelf life, solid S-SNEDDS capsules were stored in high-density polyethylene bottles at a temperature of 30 ± 0.5 °C, 40 ± 0.5 °C, and 50 ± 0.5 °C with ambient humidity conditions up to a period of 3 months. Samples were withdrawn at a specific time interval (0, 1, 2, and 3 months) and the drug content was determined by HPLC. Zero time samples were used as control. The kinetics of ezetimibe degradation were determined. The reaction rate constant (K) for the degradation was measured from the slope of lines at each elevated temperature, and an Arrhenius plot constructed (i.e., Plot between $\log K$ at various elevated temperatures and the reciprocal of absolute temperature). From the plot, K value at 25 °C (K_{25}) was used for prediction of shelf life by substituting in Eq. (2).

$$t_{0.9} = 0.1052/K_{25} \quad (2)$$

where $t_{0.9}$ is the time required for 10 % degradation of the drug and is referred to as shelf life.

Results and discussion

Solubility study and selection of oil

The drug loading capability is the main factor that needs to be considered during selection of oil. The drug loading potential of the self-emulsifying formulation is directly proportional to the drug solubility in the oily phase (Pouton

2000). The saturation solubilities (Mean \pm SD, $n = 3$) of ezetimibe in long chain triglycerides (LCT) such as Castor oil, Coconut oil, and Olive oil were found to be 2.85 ± 0.12 , 1.19 ± 0.04 and 0.58 ± 0.06 mg/ml respectively. The solubilities of ezetimibe (Mean \pm SD, $n = 3$) in the MCT/synthetic oils such as Labrafac lipophile WL1349, Labrafac PG, Captex 300, Captex 355, and Miglyol 812 N were found to be 6.35 ± 0.22 , 5.96 ± 0.11 , 6.51 ± 0.24 , 7.82 ± 0.19 and 5.04 ± 0.16 mg/ml respectively. It was observed that the solubility of ezetimibe was significantly higher in synthetic oils/MCT in comparison with the natural oils. This might be due to the shorter chain length and better fluidity of MCT over LCT (Pouton and Porter 2008). In this study, Captex 355 was chosen as the oily phase for formulating the SNEDDS.

Selection of surfactant

Only hydrophilic surfactants ($\text{HLB} > 12$) were screened, as this will favor the formation of an oil-in-water emulsion under Type-III A lipid based classification system as proposed by Pouton (2000). A type-III A system favors the formation of SNEDDS that undergoes complete emulsification to produce an optically clear dispersion having droplet size below 100 nm (Mohsin et al. 2009; Pouton 2000). Moreover, only non-ionic surfactants were used in this study because of less toxicity, as compared to the ionic one (Bali et al. 2011). The results for surfactant screening are shown in Table S1 (Online Resource). Cremophor RH40, Solutol HS15, and Labrasol formed a spontaneous dispersion. In case of Cremophor EL and Tween 80, the resulting dispersions formed a crystalline gel that was difficult to disperse. Out of all the surfactant screened, Cremophor RH40 exhibited highest emulsifying ability. The dispersion obtained from Cremophor RH40 required a minimum number (10) of flask inversion and found to possess a higher transmittance (94.8 %), lower turbidity (95 NTU) as compared to the dispersion obtained from the rest surfactants. Cremophor RH40 with an average HLB of 15 has an inhibitory effect on P-gp (Basalious et al. 2010) and reported to improve the bioavailability of some poorly soluble drugs formulated as self-emulsifying formulations, such as Silybin (Wei et al. 2012), Halofantrine (Thomas et al. 2012), Seocalcitol (Grove et al. 2007). Moreover, Cremophor RH40 has been used in commercial products such as Neoral[®] and Kaletra[®] (Strickley 2007). In this study, Cremophor RH40 was selected as the surfactant due to its highest emulsifying property.

Selection of co-surfactant

The result obtained from the co-surfactant screening was presented in Table S2 (Online Resource). Among the screened co-surfactants, Imwitor 988 and Capmul MCM

exhibited better emulsifying abilities owing to their ability to form a spontaneous dispersion. In case of Capmul PG8 and PEG 400, the dispersion proceeded through an intermediate crystalline phase transition. The dispersions obtained were found to be of less turbid in case of Imwitor 988 (97.7 % transmittance, 83 NTU) as compared with Capmul MCM (94.1 % transmittance, 103 NTU), Capmul PG8 (93.1 % transmittance, 184 NTU), PEG 400 (92.5 % transmittance, 220 NTU). Moreover, in case of Imwitor 988, it took a minimum number of flask inversions (03) to form a homogenous emulsion. The results clearly suggested that the lipophilic co-surfactant like Imwitor 988 and Capmul MCM holds a better emulsifying ability than the hydrophilic co-surfactant such as PEG 400 and Capmul PG8 containing hydrophilic glycol moieties. This might be due to the better miscibility of lipophilic co-surfactant with the MCT, which promotes self-emulsification more effectively (Pouton and Porter 2008). Moreover, the better self-emulsifying property of Imwitor 988 over Capmul MCM might be due to its structure. Imwitor 988 (a mono- and di-caprylic acid ester of glycerol) has a shorter carbon chain length as compared to Capmul MCM (mono- and di-caprylic acid and capric acid ester of glycerol). Co-surfactants with a shorter molecular chain length are considered more efficient as they can easily penetrate into the interface. This in turn enhances the water penetration into the interface and subsequently, increasing the interfacial fluidity for spontaneous emulsion formation (Pouton 2000).

Ternary phase diagram studies

To identify the region of nanoemulsion, a ternary phase diagram was constructed in an absence of the drug for the selected oil, surfactant and co-surfactant (Basalious et al. 2010). The ternary phase diagram is shown in Fig. S1 (Online Resource). The outer parallelogram denotes the area that was explored for finding the nanoemulsion regions (blue colored). It was observed that a milky or turbid emulsion was obtained either at a higher (>60 parts w/w) or lower (<20 parts w/w)

concentration of Captex 355 and Cremophor RH40. The spontaneity of emulsion formation was increased by an increase in Imwitor 988 concentrations (up to 30 parts w/w). The region of nanoemulsion was appeared between the combination of Captex 355 (20–60 parts w/w), Cremophor RH40 (20–60 parts w/w), and Imwitor 988 (10–30 parts w/w).

Optimization of SNEDDS preconcentrate using experimental design

Following ternary phase diagram studies, a circumscribed CCD was employed for the systematic optimization of the SNEDDS. The levels of oil, surfactant, and co-surfactant employed in the design were based on the results of phase diagram studies. The factors along with the optimization goal are summarized in Table 1, whereas the results obtained after execution of the experimental plan are presented in Table S3 (Online Resource).

Influence of factors on mean droplet size

The droplet size is a crucial parameter for assessing the performance of self-emulsifying formulation as a smaller droplet size provides a larger interfacial area that permits a faster drug release (Pund et al. 2014). It can be observed from the response surface plot (Fig. 1a) that initially, the mean droplet size tends to decrease with an increase in the concentration of both Captex 355 and Cremophor RH40. However, beyond 40 % w/w of Captex 355, the mean droplet size was increased in spite of increasing Cremophor RH40 concentration. From Fig. 1b, it can be observed that within 40 % w/w of Cremophor RH40 concentration, the mean droplet size was decreased gradually with an increase in Imwitor 988 concentrations. However, the mean droplet size was increased at a combination of both Cremophor RH40 (>40 % w/w) and Imwitor 988 (>30 % w/w). The regression equation obtained from the mean droplet size (Y1) is as below Eq. (3).

Table 1 Concise circumscribed central composite design for three-factor along with optimization goal

| Factors | Levels used (parts w/w) | | | | |
|----------|-------------------------|-------|-------|-------|----------------------|
| | −1.682 (− α) | −1 | 0 | +1 | +1.682 (+ α) |
| X1 | 6.36 | 20.00 | 40.00 | 60.00 | 73.64 |
| X2 | 6.36 | 20.00 | 40.00 | 60.00 | 73.64 |
| X3 | 3.83 | 10.00 | 20.00 | 30.00 | 36.82 |
| Response | Goal | | | | |
| Y1 | Minimize (<100 nm) | | | | |
| Y2 | Minimize (<20 NTU) | | | | |
| Y3 | Maximize (>99 %) | | | | |

X1 Captex 355, X2 Cremophor RH40, X3 Imwitor 988, Y1 mean droplet size (nm), Y2 turbidity (NTU), Y3 transmittance (%)

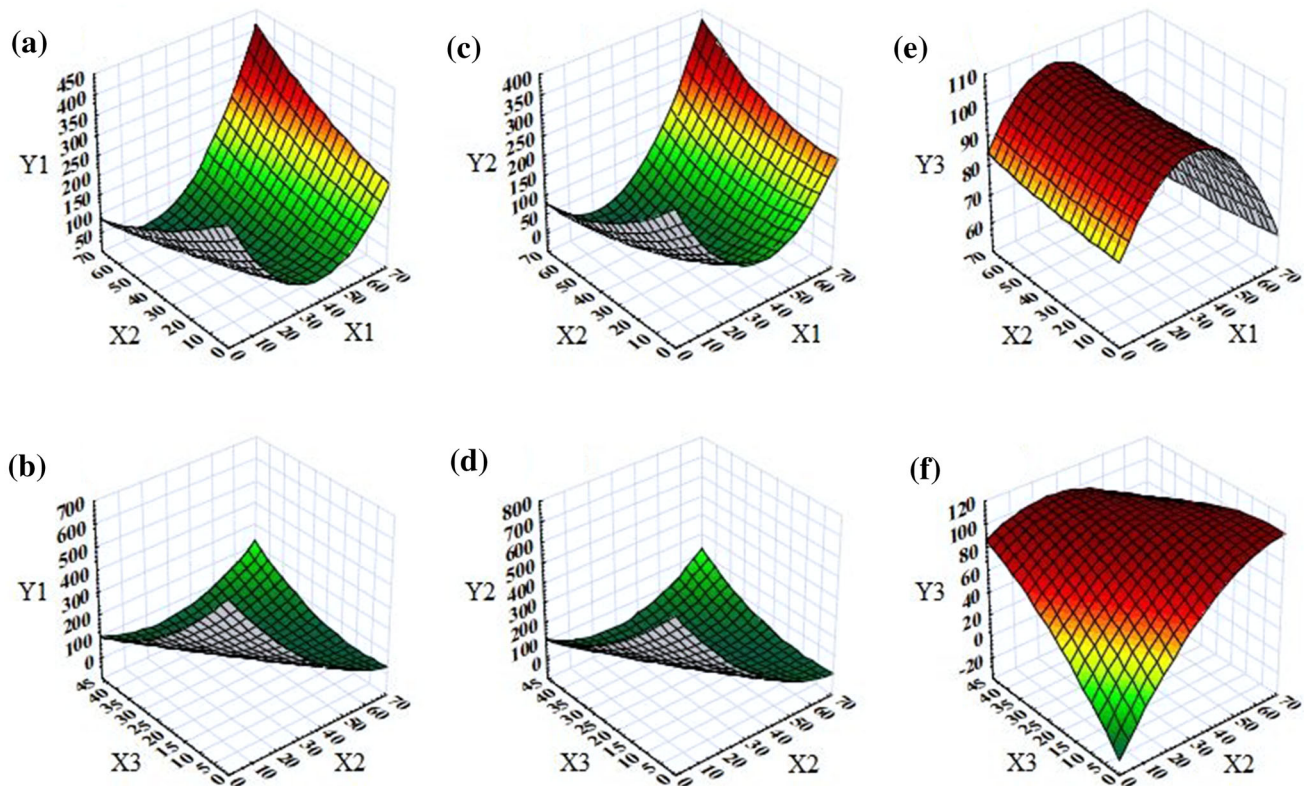


Fig. 1 Response surface plots for mean droplet size (nm) (Y1) (a, b); turbidity (NTU) (Y2) (c, d) and transmittance (%) (Y3) (e, f). X1 Captex 355 (% w/w), X2 Cremophor RH40 (% w/w), X3 Imwitor 988 (% w/w)

$$\begin{aligned}
 Y1 = & 64.2066 + 3.9525(X1) - 2.9396(X2) - 2.4340(X3) \\
 & + 0.0267(X1)^2 + 0.0311(X2)^2 + 0.0501(X3)^2 \\
 & - 0.0592(X1.X2) - 0.1001(X1.X3) + 0.0668(X2.X3)
 \end{aligned}
 \quad (3)$$

The mean droplet size of diluted SNEDDS preconcentrates was varied between 23.6 and 241.2 nm. Pareto chart (Fig. 2a) shows the linear (X1) as well as quadratic (X1)² effects of Captex 355 were having significant ($p < 0.05$; Table S4, Online Resource) effect on the mean droplet size. Moreover, the positive coefficients associated with these model terms (+3.9525 for X1, and +0.0267 for X1²; Eq. 3), implies that an increase in Captex 355 concentration, increased the mean droplet size. MCT such as Captex 355 increases surface tension at the oil/water interface leading to the coarser and aggregated droplets (Pouton and Porter 2008). The linear (X2) effect of Cremophor RH40 had a significant ($p < 0.05$; Table S4, Online Resource) effect on the mean droplet size. The negative coefficient of the model term (X2) (−2.9396; Eq. 3) indicates an antagonistic effect that decreased the mean droplet size with an increase in Cremophor RH40 concentration. Surfactant reduces surface tension at the oil/water interface that leads to lowering of the free energy required to form an emulsion.

In addition, surfactant stabilizes oil droplets by forming a barrier to coalescence (Gursoy and Benita 2004). A significant ($p < 0.05$; Table S4, Online Resource) negative interaction (a decrease in mean droplet size) was observed between Captex 355 and Cremophor RH40 (X1X2). This signifies Cremophor RH40 successfully counteracted the interfacial tension raised by Captex 355, which in turn decreases the droplet size. Further, the interaction term (X1X2) had the most profound effect on the mean droplet size due to its highest bar length observed in the Pareto chart (Fig. 2a). However, the quadratic effect of Cremophor RH40 (X2)² found to be significant ($p < 0.05$; Table S4, Online Resource) with a positive coefficient (an increase in mean droplet size) (Eq. 3). This phenomenon could be due to more water penetration into the oil droplets mediated by the excess of surfactant. This may be due to the breaking the interfacial surface of the oil droplets that leads to the coarser emulsions (Gursoy and Benita 2004). The linear effect of Imwitor 988 (X3) was found to be not significant indicates co-surfactant by itself does not possess any emulsifying ability. But it increases interfacial fluidity by enhancing water penetration into the oil/water interface (Pund et al. 2014). The co-surfactant effect was verified due to the interaction that observed between Captex 355 and Imwitor 988 (X1X3), which

decreased the mean droplet size, indicating the ability of Imwitor 988 to counteract the effect of Captex 355 (negative interaction). This in turn caused enhanced water penetration into the interface, thus providing more flexibility for the rupturing of liquid crystalline phase needed for spontaneous emulsification. The average difference between observed and predicted mean droplet size was found to be 9.4 nm, with the largest difference of 27.1 nm.

Influence of factors on turbidity

Turbidity expressed in NTU can be used as an indirect measure of emulsion droplet size due to the existence of a direct correlation between the intensity of the scattered light and volume of dispersed droplets (Nazzal and Khan 2002). It can be observed from Fig. 1c, that the turbidity was decreased with a gradual increase in Captex 355 concentrations (up to 40 % w/w). However, beyond 40 % w/w of Captex 355, the turbidity was increased in spite of an increase in surfactant (Cremophor RH40) concentration. From Fig. 1d, it can be seen that a decrease in turbidity was observed with an increase in concentrations of Cremophor RH40 as well as Imwitor 988. However, at a higher concentration (above 50 % w/w) of Cremophor RH40, turbidity was increased even though increasing the co-surfactant (Imwitor 988) concentration. The regression

equation indicating linear, quadratic, and interaction effects of the studied factors upon turbidity (Y2) is shown below in Eq. (4).

$$\begin{aligned}
 Y_2 = & 52.5540 + 3.8359 (X_1) - 3.5249 (X_2) \\
 & - 2.8642 (X_3) + 0.0339 (X_1)^2 + 0.0437 (X_2)^2 \\
 & + 0.0566 (X_3)^2 - 0.0747 (X_1.X_2) - 0.0929 (X_1.X_3) \\
 & + 0.0671 (X_2.X_3) \tag{4}
 \end{aligned}$$

It can be noticed from the Pareto chart (Fig. 2b) and statistical data of ANOVA (Table S4, Online Resource) that all model terms (except the linear and quadratic effect of Imwitor 988) had a significant ($p < 0.05$; Table S4, Online Resource) effect on turbidity. The negative interaction (a decrease in NTU) between Captex 355 and Cremophor RH40 (X1X2) had the most significant influence on turbidity (Fig. 2b). The turbidity of the diluted SNEDDS preconcentrates was found to be within the range of 6.5-214.3 NTU. The average difference between observed and predicted turbidity was found to be 7.57 NTU while the largest difference was 22 NTU. The results indicated that the significance of all the model terms (except the interaction between Cremophor RH40 and Imwitor 988) upon turbidity were similar to their observed effect on the mean droplet size. A good correlation ($r^2 = 0.977$) was observed between turbidity and mean droplet size.

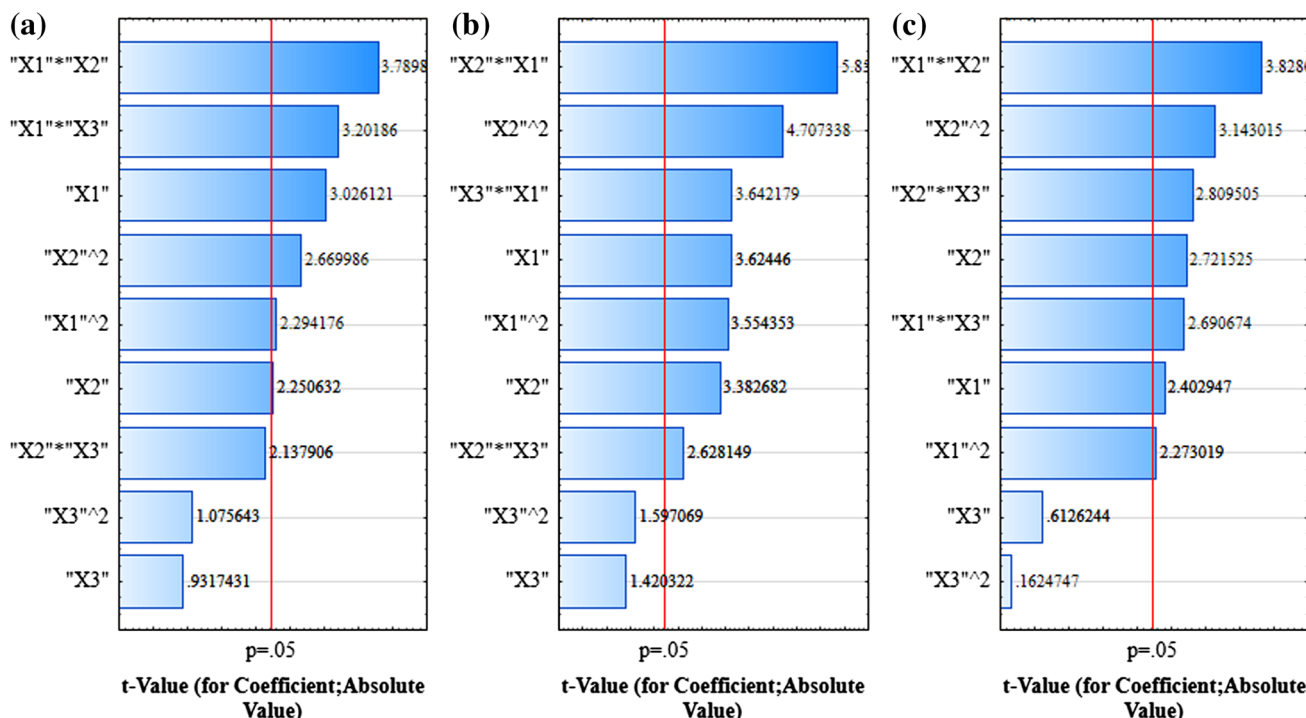


Fig. 2 Pareto charts for mean droplet size (nm) (a), turbidity (NTU) (b) and transmittance (%) (c). X1 Captex 355 (% w/w), X2 Cremophor RH40 (% w/w), X3 Imwitor 988 (% w/w)

Influence of factors on percentage transmittance

Since nanoemulsion is optically isotropic and thermodynamically stable solution, percentage transmittance studies are important to meet its isotropic parameters (Rahman et al. 2012). Percentage transmittance closer to 100 % implies that droplet size of the nanoemulsion approximates the nanometer range, which can generate a large surface area for the enhanced release and absorption of drugs (Bali et al. 2011). In our studies, it can be seen from Fig. 1e, that the percentage transmittance (Y3) was increased by an increase in concentration (up to 30 % w/w) of Captex 355. However, the percentage transmittance was decreased with a further increase (>30 %w/w) in the concentration of Captex 355. Percentage transmittance was increased by an increase in both Cremophor RH40 as well as Imwitor 988 concentrations (Fig. 1f). The regression equation obtained for percentage transmittance is shown in Eq. (5).

$$Y3 = 90.4305 - 0.7395(X1) + 0.8375(X2) + 0.3771(X3) - 0.0062(X1)^2 - 0.0086(X2)^2 - 0.0018(X3)^2 + 0.0141(X1.X2) + 0.0198(X1.X3) - 0.0207(X2.X3) \quad (5)$$

The observed transmittance for diluted SNEDDS preconcentrate was found to be within 60.0–99.9 %. From Pareto chart (Fig. 2c) and ANOVA (Table S4, Online Resource), it can be observed that all model terms (except linear and quadratic effects of Imwitor 988) had a significant ($p < 0.05$; Table S4, Online Resource) effect upon percentage transmittance. The positive interaction between Captex 355 and Cremophor RH40 (X1X2) was the most significant ($p < 0.001$) model term affecting percentage transmittance. The average and largest differences between observed and predicted transmittance were 2.2 and 6.2 % respectively. From these results, it can be inferred that the effects of these model terms upon percentage transmittance were similar to the effect that observed on mean droplet size but in an opposite direction. A good correlation ($r^2 = 0.939$) was observed between percentage transmittance and mean droplet size.

Derringer's desirability and optimization of SNEDDS preconcentrate

Both graphical and numerical methods were employed to optimize the SNEDDS preconcentrate. The criterion for optimum SNEDDS preconcentrate was based on the highest possible values of response, namely percentage transmittance (>99 %), and lowest possible values of responses such as droplet size (<100 nm) and turbidity (<20 NTU). Under these conditions, the desirability (d) for each response can be combined to get global desirability

(D), which can be used to get an optimum combination of factors (Derringer and Suich 1980). The global desirability can be represented as below in Eq. (6).

$$D = [d_1^{p_1} \times d_2^{p_2} \times \dots \times d_n^{p_n}]^{1/n} \quad (6)$$

where, d_i is the individual desirability function of each response, n is the number of response and p_i is the weight of the response. The scale of d_i varies between 0 (undesired response) and 1 (fully desired response). A value of D close to 1 signifies response values are close to the target values. The advantage of this function is that if the criteria for any responses fall outside the desirable range, then the overall product will be unacceptable. The present goal of this study was to minimize mean droplet size and turbidity, and to maximize percentage transmittance. The weight of the responses (p) was set to 1. Out of several combinations tried, the global desirability was found to be 0.99 (Fig. S2, Online Resource), which is very close to 1 for the optimal SNEDDS preconcentrate that consisted of Captex 355 (30 % w/w), Cremophor RH40 (40 % w/w) and Imwitor 988 (30 % w/w). The graphical representations of desirability for individual responses were presented in Fig. S3 (Online Resource) and found to be in a good agreement with the above conditions predicted by the numerical method. The mean droplet size, turbidity, and percentage transmittance of the diluted optimized SNEDDS preconcentrate were found to be 34.6 ± 0.45 nm, 4.8 ± 0.1 NTU, and 99.6 ± 0.02 respectively ($n = 3$). Thus, satisfies the optimization goals.

Validation and adequacies of the models

The ANOVA results (Table S4, Online Resource) clearly depict a high F value (16.07 for Y1, 28.41 for Y2 and 11.30 for Y3) along with a low “p” value ($p < 0.001$) indicates the significance of the models. The relationships between the observed and predicted responses were found to be linear and acceptable, as the adjusted R^2 was higher than the recommended limit (for chemical samples) of 0.8 (0.8771 for Y1, 0.9285 for Y2 and 0.8299 for Y3) (Lundstedt et al. 1998). The adequacy of the models was examined by the inspection of residuals. The difference between the observed and predicted values of a response is regarded as residual. As shown in Fig. S4 (Online Resource), the residual analysis demonstrated no obvious pattern. The residuals for each response were found to be randomly distributed with an almost equal scatter above and below the zero-line of the residual graph. Moreover, the normal probability plots (Fig. S5, Online Resource) and histograms of residuals (Fig. S6, Online Resource) were inspected, where the residuals were found to be normally distributed and satisfied the normality assumption of residuals. This suggests that the models are adequate and

the experimental measurement's variance being constant for all responses (Montgomery 2013).

Loading of drug in SNEDDS preconcentrate

The saturation solubilities (Mean \pm SD, $n = 3$) of ezetimibe in water and optimized SNEDDS preconcentrate were found to be 0.0120 ± 0.0014 mg/ml and 90.62 ± 1.15 mg/ml respectively. This enhancement in solubility of ezetimibe was 7552-fold and was extremely significant ($p < 0.001$) in comparison to its aqueous solubility. In order to solubilize ezetimibe within a short mix-up time, it was loaded at 90 % saturation solubility level (~ 80 mg/ml) in the optimized SNEDDS preconcentrate.

Characterization of liquid S-SNEDDS

Thermodynamic stability studies

Emulsions are thermodynamically unstable systems, but nanoemulsions are highly stable systems without phase separation, creaming, cracking, and differentiate it from the micro-emulsion (Rahman et al. 2012). Liquid S-SNEDDS was examined for centrifugation, heating–cooling cycles and passed these tests. No phase separation, creaming, and cracking were observed. The cloud point of liquid S-SNEDDS was found to be within 88–90 °C. This indicates the nanoemulsion formed at the physiological temperature (37 °C) will be a stable one (Bali et al. 2011).

Droplet size and zeta potential analysis

The mean droplet sizes of liquid S-SNEDDS were found to be within 27.0–34.8 nm. The mean droplet size of the liquid S-SNEDDS (containing 5 % w/w HPMC-E5) was found to be 27.3 nm (Fig. 3a) and was significantly ($p < 0.05$) smaller than the mean droplet size of diluted SNEDDS preconcentrate (34.6 nm) or diluted liquid SNEDDS (without HPMC-E5) (34.8 nm). This reduction in mean droplet size of the diluted liquid S-SNEDDS might be due to the presence of HPMC-E5, which forms a physical barrier around oil droplets and prevented it from the aggregation (Wei et al. 2012).

Zeta potentials of the diluted liquid S-SNEDDS (with or without HPMC-E5) were found to be ranging from -0.4 to -0.5 mV. This indicates HPMC-E5, being a nonionic polymer, had no role in affecting zeta potential. The negative charge of the zeta potential indicates a kinetically stable nanoemulsion due to the anionic groups of the fatty acids and glycols present in the oil, surfactant and co-surfactant (Bali et al. 2011; Pund et al. 2014).

Measurement of transmittance and turbidity

The dispersions obtained from the liquid S-SNEDDS were found to be clear and transparent. The observed turbidities and transmittance were ranged between 4.5 and 4.9 NTU and 99.5–99.9 % respectively.

Transmission electron microscopy

Transmission electron microscopy image of diluted liquid S-SNEDDS (with 5 % w/w HPMC-E5) is shown in Fig. 3b. The droplets were appeared to be un-coagulated, spherical, having droplet size below 30 nm and found to be in good agreement with the droplet size as analyzed by DLS.

Characterization of solid S-SNEDDS

Micromeritic properties

The flow properties of solid S-SNEDDS were found to be good and were within the acceptable limits as mentioned below. The Carr's index, Hausner's ratio, and angle of repose were ranged between 18–20.5, 1.22–1.25, and 25–29 respectively.

In vitro supersaturation test and selection of PPI concentration

In order to find out the apparent ezetimibe concentration following dilution of solid S-SNEDDS, an in vitro precipitation test was designed. The total volume of the medium chosen was 100 ml, which was equal to the volume of the residual stomach fluid (20–50 ml) in a fasted state and the amount of water (30–60 ml) administered during ingestion of the dosage form. The existence of ezetimibe within the media can be confined to three different states such as the free molecules in solution (*state 1*), solubilized molecule partitioned into nanoemulsion (*state 2*), and molecule precipitated into solid particles (*state 3*) (Gao et al. 2009). The transfer of ezetimibe between above states changes rapidly over time. The use of 0.45 μ m filter to process test samples aimed to exclude precipitated ezetimibe, but allowing the free ezetimibe molecule and nanoemulsion globules. Hence, the total concentration of ezetimibe measured was the summation of *state 1* and 2 rather than free ezetimibe (*state 1*) alone. Figure 4a depicts the apparent ezetimibe concentration–time profile, where ezetimibe concentration dropped down rapidly within initial 5 min. However, the precipitation of ezetimibe was retarded in the formulation containing HPMC-E5, with a maximum retard (at least up to 60 min) being observed at

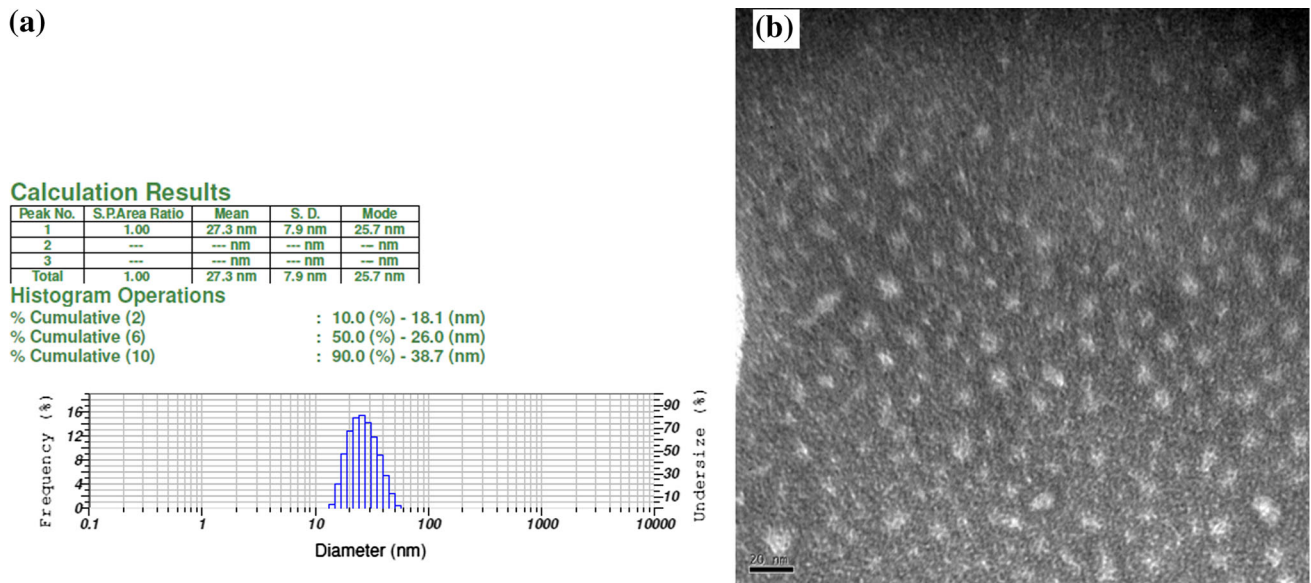


Fig. 3 **a** Dynamic light scattering data of the liquid S-SNEDDS (500 times diluted with water); **b** Transmission electron microscopy image of the liquid S-SNEDDS (500 times diluted with water), bar length represent 20 nm

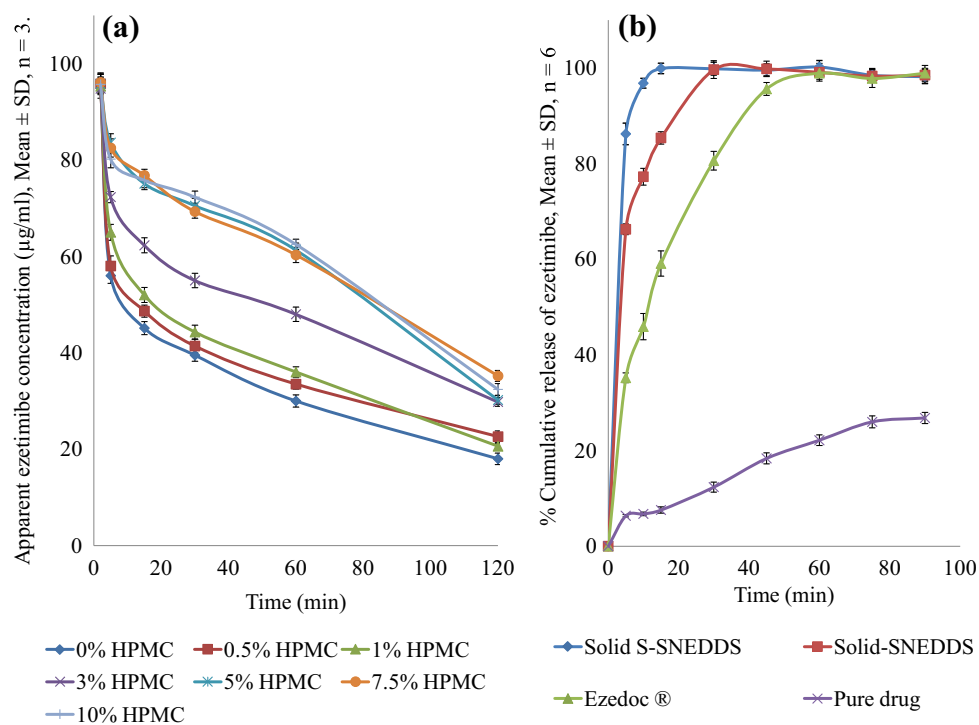


Fig. 4 **a** Apparent concentration–time profile of ezetimibe from in vitro supersaturation test of solid S-SNEDDS containing variable amount of HPMC-E5; **b** In vitro release profiles for the solid S-SNEDDS, solid SNEDDS, commercial tablet (Ezedoc®) and ezetimibe (alone)

5 % w/w HPMC-E5. Apparent concentration–time profile of ezetimibe was found to be unaffected (statistically insignificant) with a further increase (>5 % w/w) in HPMC-E5 concentration. Hence, at 5 % w/w level HPMC-E5 was selected to incorporate within the optimized SNEDDS preconcentrate. HPMC at a small concentration,

adsorb onto hydrophobic nuclear surface and act as a barrier for nucleation process responsible for the crystallization. This in turn retards excessive drug precipitation out of the solution to maintain a supersaturated state (Brouwers et al. 2009; Gao et al. 2009). Earlier reports indicate that among HPMC polymers, hydrophobic E-type

(29 % methyl substitution) adsorbs better to the hydrophobic nuclei and are better precipitation inhibitors than their less hydrophobic counterparts K-type (22 % methyl substitution). In contrast, a hydrophilic polymer like polyvinyl pyrrolidone (PVP K30) remained an inactive precipitation inhibitor (Gao et al. 2009). Moreover, between HPMC-E type polymer, the effectiveness of a lesser viscous HPMC-E5 (5 mPa.s) was found to be superior as compared to other higher viscosity grades such as HPMC-E4 M (4000 mPa.s), HPMC-E50 (50 mPa.s), and HPMC-E15 (15 mPa.s) (Bandyopadhyay et al. 2014; Gao et al. 2009).

Powder XRD studies

As shown in Fig. 5a, X-ray diffractogram of ezetimibe exhibited several sharp peaks similar to the one reported earlier by Bandyopadhyay et al. 2014. The physical mixture (Fig. 5b) showed all the characteristic peaks of ezetimibe and excipients. Microcrystalline cellulose (Fig. 5f) and HPMC-E5 (Fig. 5h) did not show any prominent peaks, whereas talc (Fig. 5g) showed two strong, sharp peaks at 9.5° and 28.7° that appeared in the solid S-SNEDDS blank, precipitates obtained from the in vitro supersaturation test (Fig. 5c and d) and physical mixture (Fig. 5b). A decrease in crystallinity of ezetimibe in the solid S-SNEDDS precipitates (with or without HPMC-E5) was observed compared to the free drug (powder). However, the precipitate obtained from the solid S-SNEDDS containing 5 % w/w HPMC-E5 (Fig. 5d) was completely amorphous lacking characteristic peaks of ezetimibe at 18.7° , 19.4° in contrast to the partially amorphous precipitate obtained from the formulation having 0 % HPMC-E5

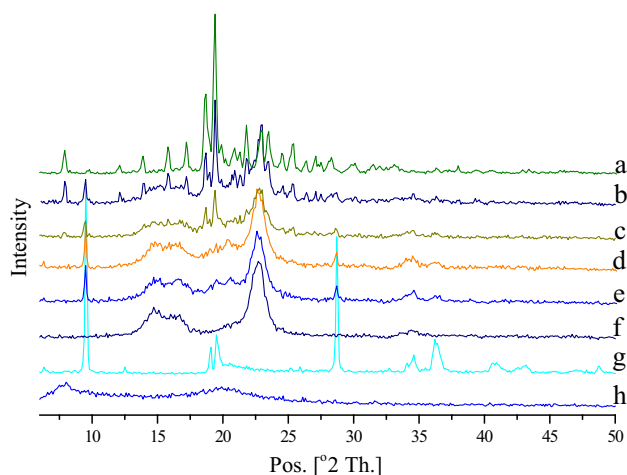


Fig. 5 Powder X-ray diffractogram of **a** ezetimibe (alone); **b** physical mixture of ezetimibe and solid S-SNEDDS blank; **c** precipitates of solid S-SNEDDS (0 % HPMC-E5); **d** precipitates of solid S-SNEDDS (5 % HPMC-E5); **e** solid S-SNEDDS blank; **f** microcrystalline cellulose; **g** talc and **h** HPMC-E5

(Fig. 5c). This suggests that, ezetimibe was precipitated in a complete amorphous state from solid S-SNEDDS containing HPMC-E5 (at 5 % w/w).

Differential scanning calorimetry

The DSC thermograms of ezetimibe, solid S-SNEDDS, solid S-SNEDDS blank, physical mixture, and individual excipients are presented in Fig. 6. Pure ezetimibe showed a sharp endothermic peak at 165.74°C (Fig. 6a). In case of the physical mixture, an endothermic peak due to ezetimibe with reduced intensity was observed (Fig. 6b). Solid S-SNEDDS (Fig. 6c) and solid S-SNEDDS blank (Fig. 6d) did not show any characteristic peaks of ezetimibe. Moreover, microcrystalline cellulose (Fig. 6e), talc (Fig. 6f), and HPMC-E5 (Fig. 6g) did not show any peak in the melting point region of ezetimibe. The results suggest that ezetimibe crystals were present in a changed amorphous state within the solid S-SNEDDS.

Scanning electron microscopy

The surface and cross-sections of ezetimibe, solid S-SNEDDS, solid S-SNEDDS blank and physical mixtures were studied by SEM. As presented in Fig. 7a, ezetimibe was appeared as smooth surfaced, needle shaped, and isolated crystals. These characteristics ezetimibe crystals can be seen in the physical mixture (Fig. 7d). However, solid S-SNEDDS appeared as rough surfaced agglomerated particles having no distinct ezetimibe crystals on its surface (Fig. 7b). Moreover, the surface of solid S-SNEDDS was found to be in close resemblance to the surface of solid S-SNEDDS blank (Fig. 7c). Our results suggested that

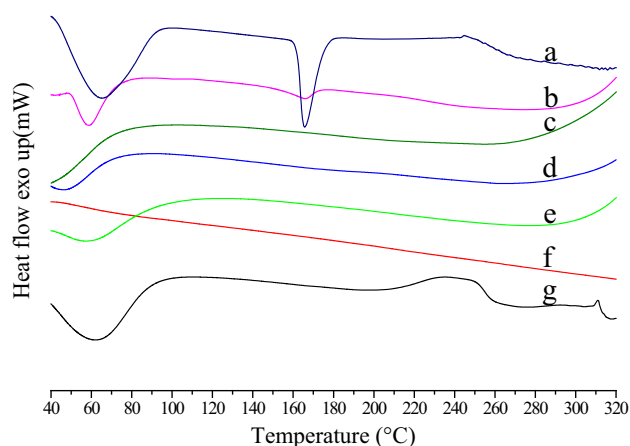


Fig. 6 Differential scanning calorimetric thermograms of **a** ezetimibe (alone); **b** physical mixture of ezetimibe and solid S-SNEDDS blank; **c** solid S-SNEDDS; **d** solid S-SNEDDS blank; **e** microcrystalline cellulose; **f** talc and **g** HPMC-E5

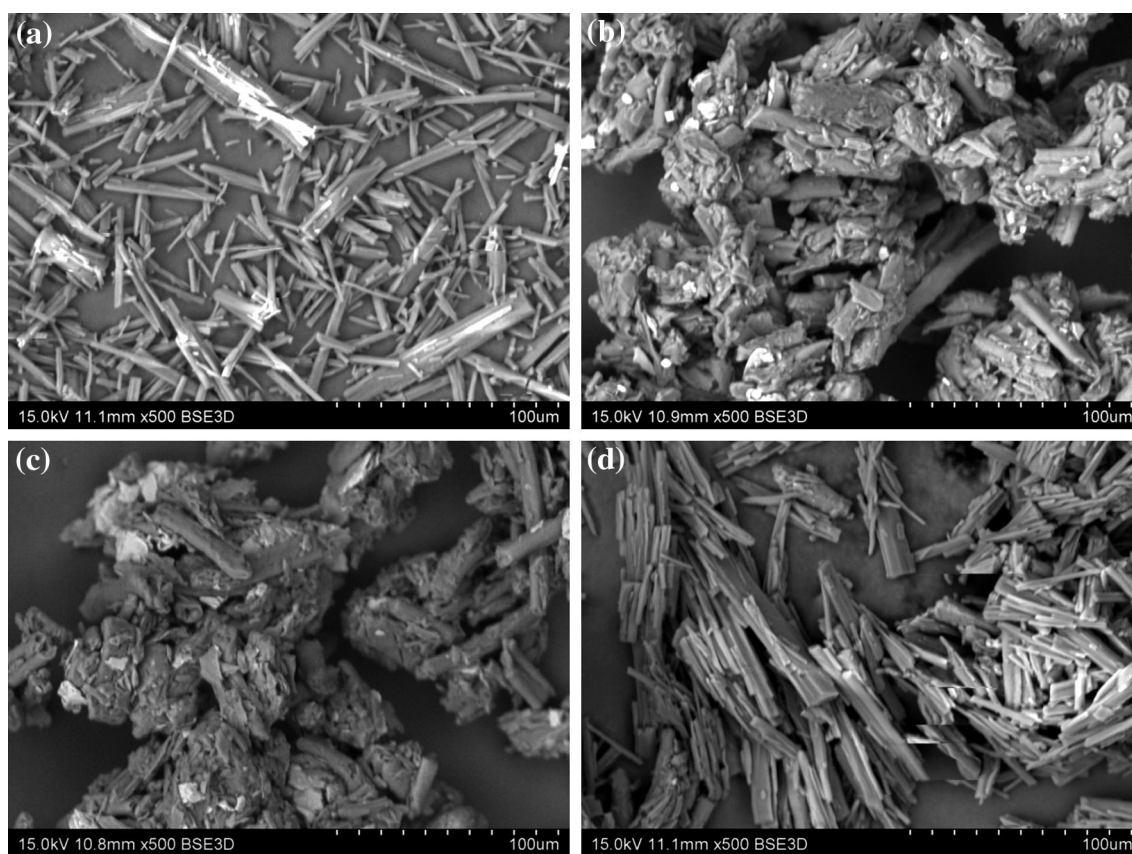


Fig. 7 Scanning electron microscopic images of **a** ezetimibe (alone); **b** solid S-SNEDDS; **c** solid S-SNEDDS blank and **d** physical mixture of ezetimibe and solid S-SNEDDS blank

ezetimibe was dissolved in a molecular level inside the pores of the solid S-SNEDDS matrix.

Fourier transformed infrared (FTIR) spectroscopy

The FTIR spectra of pure ezetimibe (Fig. S7a, Online Resource) showing characteristic peaks at 3269.61 cm^{-1} (O–H str), 2919.09 cm^{-1} (C–H str), 1879.92 cm^{-1} (lactone ring C=O str), 1718.22 cm^{-1} (C=O str), 1509.9 cm^{-1} (C=C str), 1445.68 cm^{-1} (C–N str), 1403.46 and 1272.24 cm^{-1} (C–F str), 1220.89 cm^{-1} (C–O str) and 831.15 cm^{-1} (ring vibration of para substituted benzene ring). The above peaks due to ezetimibe can be clearly observed in physical mixture (Fig. S7b, Online Resource) and in solid S-SNEDDS (Fig. S7c, Online Resource). No substantial shifting of functional group position occurred in the case of solid S-SNEDDS indicating no major interaction of ezetimibe with solid excipients.

Comparative in vitro dissolution studies

A significant ($p < 0.001$) increase in the ezetimibe release was observed from the solid S-SNEDDS ($DR_{15\text{ min}} = 99.89\%$) vis-à-vis solid SNEDDS (85.36%), Ezedoc[®]

(59.19%) and the free drug (powder) (7.55%) (Fig. 4b). This increase in $DR_{15\text{ min}}$ in case of solid S-SNEDDS was 1.17, 1.69, and 13.21-fold higher as compared with the $DR_{15\text{ min}}$ values of solid-SNEDDS, Ezedoc[®], and the free drug (powder), respectively. Initially, solid S-SNEDDS showed a higher drug release (20–25%) as compared with the solid SNEDDS. This could be due to the presence of HPMC-E5 within solid S-SNEDDS that resisted the excessive precipitation of ezetimibe as evident from the result of in vitro supersaturation study. Moreover, as confirmed from the PXRD studies, the precipitate obtained in presence of HPMC-E5 was found to be completely amorphous than the precipitate obtained in an absence of it. HPMC-E5 employed as PPI, adsorbed onto the hydrophobic surface of nuclei, acted as a barrier for nucleation process, inhibited the formation of crystals and growth rate of crystallization of ezetimibe (Brouwers et al. 2009; Gao et al. 2009). Amorphous forms require less energy to dissolve, resulting in higher apparent solubilities and dissolution rates. In addition, the superior drug release from the solid S-SNEDDS might be attributed to the presence of ezetimibe in a molecularly dissolved state as confirmed from DSC, and SEM analysis. Since the drug is molecularly dissolved within the matrix of solid

Table 2 Data obtained from accelerated stability studies of ezetimibe solid S-SNEDDS

| Time (month) | Ezetimibe content (%) ^a | DR _{15 min} (%) ^{a, b} | Droplet size (nm) ^a | Similarity factor (<i>f</i> ₂) ^a |
|--------------|------------------------------------|--|--------------------------------|--|
| 0 | 99.96 ± 0.21 | 99.89 ± 0.52 | 27.43 ± 0.15 | – |
| 3 | 98.53 ± 0.28 | 99.29 ± 0.92 | 28.40 ± 0.26 | 97.17 ± 3.55 |
| 6 | 96.86 ± 0.51 | 99.70 ± 0.61 | 28.76 ± 0.18 | 92.61 ± 2.98 |

^a Data presented in Mean ± SD, n = 3^b Percentage of drug release at 15 min**Table 3** Data obtained during estimation of shelf life of ezetimibe solid S-SNEDDS

| Temperature (°C) | Absolute temperature (K) | Slope | r ^{2a} | K (day ⁻¹) ^b | log K | 1/T | t _{0.9} (year) ^c |
|------------------|--------------------------|-------------------------|-----------------|-------------------------------------|---------|-----------|--------------------------------------|
| 25 | 298 | 2.76 × 10 ⁻⁵ | – | 6.37 × 10 ⁻⁵ | -4.1953 | 0.0033557 | 4.53 |
| 30 | 303 | 4.65 × 10 ⁻⁵ | 0.997 | 1.06 × 10 ⁻⁴ | -3.9707 | 0.0033003 | 2.73 |
| 40 | 313 | 1.16 × 10 ⁻⁴ | 0.999 | 2.68 × 10 ⁻⁴ | -3.5719 | 0.0031949 | 1.04 |
| 50 | 323 | 3.00 × 10 ⁻⁴ | 0.998 | 6.90 × 10 ⁻⁴ | -3.1606 | 0.003096 | 0.42 |

Ea (kca mol⁻¹)^d = 18.13, A(sec⁻¹)^e = 14,571

^a Coefficient of correlation^b Observed rate constant^c Time left for 90 % potency^d Energy of activation^e Arrhenius frequency factor

S-SNEDDS, a high surface area is expected that improves wettability of the drug (Tang et al. 2008). Furthermore, smaller droplet size of the emulsion obtained in presence of HPMC-E5 provided a larger surface area for rapid drug release.

Accelerated stability studies and determination of shelf life of solid S-SNEDDS

Accelerated stability studies proved insignificant changes in mean droplet size and DR_{15 min} up to a period of 6 months (Table 2). As per ICH Q1A (R2) guidelines, the drug content within solid S-SNEEDS was found to be acceptable. There was no significant change observed in the assay values (>5 %). The similarity factors (*f*₂) (obtained at three and 6 months) were found to be within the accepted limits (≥50). The solidification process did not affect the mean droplet size, and the self-emulsifying ability was preserved in the solid S-SNEDDS. Ezetimibe followed first-order degradation kinetics at each elevated temperature studied, and the corresponding first-order plots were found to be linear having good correlation coefficients (r² ≥ 0.997). The slopes, *K*, t_{0.9} derived from individual first-order plots were presented in Table 3. Arrhenius plot was found to be linear (r² = 0.9992) having regression equation as $Y = -3962.3 X + 9.1$, *Y* is the log of rate constants (*K*), and *X* is the reciprocal of mean absolute temperature (K). Activation energy (*E*_a) and Arrhenius frequency factor (*A*) were found to be

18.13 kcal. mol⁻¹ and 14,571 s⁻¹ respectively. *K*₂₅ was found to be 6.37 × 10⁻⁵ day⁻¹ with a shelf life of 4.53 years. The results indicated that ezetimibe remained chemically stable in the solid S-SNEDDS.

Conclusion

Dilution of solid S-SNEDDS resulted in a nanoemulsion having a large surface area responsible or advantageous for enhanced solubilization and dissolution of ezetimibe. The central composite design employed in this study was shown to be beneficial in optimizing SNEDDS preconcentrate and highly predictive models obtained. The critical factors identified during this study were helpful in achieving the optimal goal. Solid S-SNEDDS was found to be stable and precipitation-resistant, and showed a significant (p < 0.001) increase in release rate of ezetimibe as compared with the solid-SNEDDS, commercial formulation, and free drug (powder). Incorporation of HPMC-E5 into solid S-SNEDDS effectively inhibited drug precipitation and consequently, maintained a supersaturated state of ezetimibe at least for 60 min. Moreover, solid S-SNEDDS led to the precipitation of ezetimibe in an amorphous form, which can be the driving force for its enhanced solubility and dissolution. Hence, this stable supersaturatable formulation having the added advantages of superior emulsifying ability may provide a useful oral solid dosage form for poorly water-soluble drug ezetimibe.

Acknowledgments This article does not contain any studies with human and animal subjects performed by any of the authors. Authors are thankful to Abitec Corp., Janesville, USA; BASF SE, Ludwigshafen, Germany; Gattefosse Corp., Saint-Priest, France, and Sasol olefins and surfactants, GmbH, Germany for providing excipients used during this study. The authors report no conflicts of interest. The authors alone are responsible for the content and writing of the paper.

References

- Bali V, Ali M, Ali J (2010) Novel nanoemulsion for minimizing variations in bioavailability of ezetimibe. *J Drug Target* 18:506–519
- Bali V, Ali M, Ali J (2011) Nanocarrier for the enhanced bioavailability of a cardiovascular agent: in vitro, pharmacodynamic, pharmacokinetic and stability assessment. *Int J Pharm* 403:46–56
- Bandyopadhyay S, Katare O, Singh B (2014) Development of optimized supersaturable self-nanoemulsifying systems of ezetimibe: effect of polymers and efflux transporters. *Expert Opin Drug Deliv* 11:479–492
- Basalious EB, Shawky N, Badr-Eldin SM (2010) SNEDDS containing bioenhancers for improvement of dissolution and oral absorption of lacidipine. I: development and optimization. *Int J Pharm* 391:203–211
- Brouwers J, Brewster ME, Augustijns P (2009) Supersaturating drug delivery systems: the answer to solubility-limited oral bioavailability? *J Pharm Sci* 98:2549–2572
- Carr RL (1965) Evaluating flow properties of solids, chemical engineering. *Chem Eng* 18:163–168
- Dabhi MR, Limbani MD, Sheth NR (2011) Preparation and in vivo evaluation of self-nanoemulsifying drug delivery system (SNEDDS) containing ezetimibe. *Curr Nanosci* 7:616–627
- Dash RN, Habibuddin M, Humaira T, Patel AA (2014) Application of quality by design for the optimization of an HPLC method to determine ezetimibe in a supersaturable self-nanoemulsifying formulation. *J Liquid Chromatogr Related Technol* 38:874–885
- Dash RN, Habibuddin M, Humaira T, Ramesh D (2015a) Design, optimization and evaluation of glipizide solid self-nanoemulsifying drug delivery for enhanced solubility and dissolution. *Saudi Pharm J* 23:528–540
- Dash RN, Mohammed H, Humaira T, Reddy AV (2015b) Solid supersaturable self-nanoemulsifying drug delivery systems for improved dissolution, absorption and pharmacodynamic effects of glipizide. *J Drug Deliv Sci Technol* 28:28–36
- Derringer G, Suich R (1980) Simultaneous Optimization of Several Response Variables. *J Qual Technol* 12:214–220
- Dixit RP, Nagarsenker MS (2008) Self-nanoemulsifying granules of ezetimibe: design, optimization and evaluation. *Eur J Pharm Sci* 35:183–192
- Gao P, Akrami A, Alvarez F, Hu J, Li L, Ma C, Surapaneni S (2009) Characterization and optimization of AMG 517 supersaturable self-emulsifying drug delivery system (S-SEDDS) for improved oral absorption. *J Pharm Sci* 98:516–528
- Grove M, Mullertz A, Pedersen GP, Nielsen JL (2007) Bioavailability of seocalcitol III. Administration of lipid-based formulations to minipigs in the fasted and fed state. *Eur J Pharm Sci* 31:8–15
- Gulsun T, Gursoy RN, Oner L (2011) Design and characterization of nanocrystal formulations containing ezetimibe. *Chem Pharm Bull (Tokyo)* 59:41–45
- Gursoy RN, Benita S (2004) Self-emulsifying drug delivery systems (SEDDS) for improved oral delivery of lipophilic drugs. *Biomed Pharmacother* 58:173–182
- Hu X, Lin C, Chen D, Zhang J, Liu Z, Wu W, Song H (2012) Sirolimus solid self-microemulsifying pellets: formulation development, characterization and bioavailability evaluation. *Int J Pharm* 438:123–133
- International conference on harmonisation of technical requirements for registration of pharmaceuticals for human use, Draft Step 4 (2003) Stability testing of new drug substances and products Q1A (R2). ICH, Geneva
- Khanfar M, Sheikh Salem M, Hawari R (2013) Formulation factors affecting the release of ezetimibe from different liquisolid compacts. *Pharm Dev Technol* 18:417–427
- Kiekens F, Eelen S, Verheyden L, Daems T, Martens J, Van Den Mooter G (2012) Use of ordered mesoporous silica to enhance the oral bioavailability of ezetimibe in dogs. *J Pharm Sci* 101:1136–1144
- Kosoglou T, Statkevich P, Johnson-Levonas AO, Paolini JF, Bergman AJ, Alton KB (2005) Ezetimibe: a review of its metabolism, pharmacokinetics and drug interactions. *Clin Pharmacokinet* 44:467–494
- Lestari Maria LAD, Ardiana F, Indrayanto G (2009) Ezetimibe. In: Brittain HG (ed) Profiles of drug substances, excipients and related methodology, 1st edn. Academic Press, London, pp 104–105
- Lundstedt T, Seifert E, Abramo L, Thelin B, Nystrom A, Pettersen J, Bergman R (1998) Experimental design and optimization. *Chemom Intell Lab Syst* 42:3–40
- Mohsin K, Long MA, Pouton CW (2009) Design of lipid-based formulations for oral administration of poorly water-soluble drugs: precipitation of drug after dispersion of formulations in aqueous solution. *J Pharm Sci* 98:3582–3595
- Montgomery DC (2013) Design and analysis of experiments. Wiley, Hoboken
- Nazzal S, Khan MA (2002) Response surface methodology for the optimization of ubiquinone self-nanoemulsified drug delivery system. *AAPS PharmSciTech* 3:23–31
- Pandya V, Patel J (2011) Formulation and evaluations of ezetimibe nanoparticles prepared by controlled nanoprecipitation and transformation into solid dosage. *Acta Pharm Sci* 53:477–488
- Parmar KR, Shar SR, Sheth NR (2011) Studies in dissolution enhancement of ezetimibe by solid dispersions in combination with a surface adsorbent. *Dissolution Technol* 8:55–61
- Patel R, Bhimani D, Patel J, Patel D (2008) Solid-state characterization and dissolution properties of ezetimibe–cyclodextrins inclusion complexes. *J Incl Phenomena Macrocycl Chem* 60:241–251
- Pouton CW (2000) Lipid formulations for oral administration of drugs: non-emulsifying, self-emulsifying and ‘self-microemulsifying’ drug delivery systems. *Eur J Pharm Sci* 11(Suppl 2):S93–98
- Pouton CW, Porter CJ (2008) Formulation of lipid-based delivery systems for oral administration: materials, methods and strategies. *Adv Drug Deliv Rev* 60:625–637
- Pund S, Shete Y, Jagadale S (2014) Multivariate analysis of physicochemical characteristics of lipid based nanoemulsifying cilostazol–quality by design. *Colloids Surf B Biointerfaces* 115:29–36
- Rahman MA, Iqbal Z, Hussain A (2012) Formulation optimization and in vitro characterization of sertraline loaded self-nanoemulsifying drug delivery system (SNEDDS) for oral administration. *J Pharm Investig* 42:191–202
- Sancheti PP, Karekar P, Vyas VM, Shah M, Pore YV (2009) Preparation and physicochemical characterization of surfactant based solid dispersions of ezetimibe. *Pharmazie* 64:227–231
- Strickley RG (2007) Currently marketed oral lipid-based dosage forms: Drug products and excipients. In: Hauss DJ (ed) Oral lipid-based formulations: enhancing the bioavailability of poorly water-soluble drugs, 1st edn. Informa Healthcare, New York, pp 1–31

- Sweetman SC (2009) *Martindale: the complete drug reference*. Pharmaceutical Press, London
- Tang B, Cheng G, Gu JC, Xu CH (2008) Development of solid self-emulsifying drug delivery systems: preparation techniques and dosage forms. *Drug Discov Today* 13:606–612
- Thomas N, Holm R, Müllertz A, Rades T (2012) In vitro and in vivo performance of novel supersaturated self-nanoemulsifying drug delivery systems (super-SNEDDS). *J Control Release* 160:25–32
- Wei Y, Ye X, Shang X, Peng X, Bao Q, Liu M, Gup M, Li F (2012) Enhanced oral bioavailability of silybin by a supersaturable self-emulsifying drug delivery system (S-SEDDS). *Colloids Surf A* 396:22–28